

Growing hydrodynamic modes in Keplerian accretion disks during secondary perturbations: Elliptical vortex effects

Banibrata Mukhopadhyay¹

1. *Institute for Theory and Computation, Harvard-Smithsonian Center for Astrophysics, 60 Garden Street, MS-51, Cambridge, MA 02138, USA*
2. *Department of Physics, Indian Institute of Science, Bangalore-560012, India*

ABSTRACT

The origin of hydrodynamic turbulence, and in particular of an anomalously enhanced angular momentum transport, in accretion disks is still an unsolved problem. This is especially important for cold disk systems which are practically neutral in charge and therefore turbulence can not be of magnetohydrodynamic origin. While the flow must exhibit some instability and then turbulence in support of the transfer of mass inward and angular momentum outward, according to the linear perturbation theory, in absence of magnetohydrodynamic effects, it should always be stable. We demonstrate that the three-dimensional secondary disturbance to the primarily perturbed disk, consisting of elliptical vortices, gives significantly large hydrodynamic growth in such a system and hence may suggest a transition to an ultimately turbulent state. This result is essentially applicable to accretion disks around quiescent cataclysmic variables, in proto-planetary and star-forming disks, the outer region of disks in active galactic nuclei, where the gas is significantly cold and thus the magnetic Reynolds number is smaller than 10^4 .

Subject headings: accretion, accretion disks — hydrodynamics — turbulence — instabilities

1. Introduction

Origin of turbulence and then the viscosity parameter α , while has been demonstrated for a hot Keplerian accretion disk by the magnetorotational instability (MRI; Balbus & Hawley 1991; Balbus, Hawley, & Stone 1996; Hawley, Balbus, & Winters 1999), is still not

¹bmukhopa@cfa.harvard.edu, bm@physics.iisc.ernet.in

well understood for cold disks, e.g. accretion disks around quiescent cataclysmic variables (Gammie & Menou 1998; Menou 2000), proto-planetary and star-forming disks (Blaes & Balbus 1994), and the outer region of disks in active galactic nuclei (Menou & Quataert 2001), even after more than three decades of the famous discovery of the α -disk (Shakura & Sunyaev 1973). These cold systems are largely neutral in charge so that the MRI driven turbulence appears to be ruled out. However, to support accretion, there must appear some sort of turbulence (most likely pure hydrodynamic in nature) and then the corresponding turbulent viscosity, as the molecular viscosity is negligible. Richard & Zahn (1999) indeed showed by analyzing results of laboratory experiments for the classical Couette-Taylor flow that in the case where angular momentum increases outward, similar to the Keplerian flow, hydrodynamic turbulence may be sustained. Then they derived the corresponding turbulent viscosity which is very useful for the astrophysical purpose. Longaretti (2002) argued that the Keplerian accretion flow in the shearing sheet limit should be turbulent and the lack of turbulence in simulations is due to lack of their resolution. Then Lesur & Longaretti (2005) showed that the required resolution is not possible to achieve with the presently available computer resources. They also found that the efficiency of turbulent transport is directly correlated to the critical Reynolds number for the transition to turbulence. In spite of all these analyzes, the actual origin of hydrodynamic turbulence in such systems still remains unclear. It is important to note that the numerical simulation has never been carried out with a *very high* Reynolds number what the real accretion disk exhibits. Therefore, the hydrodynamic effects may compete with the magnetohydrodynamic effects (essentially MRI) at a high Reynolds number and, in a realistic system, turbulence may be due to hydrodynamic effects independent of whether the disk is cold or hot.

Recently, several authors including ourselves have put their efforts in achieving progress toward the solution of this difficult problem (e.g. Tevzadze et al. 2003; Chagelishvili 2003; Umurhan & Regev 2004; Yecko 2004; Mukhopadhyay, Afshordi & Narayan 2005; Afshordi, Mukhopadhyay & Narayan 2005; Johnson & Gammie 2005; Umurhan et al. 2006; Barranco & Marcus 2005; Papaloizou 2005). The main aim of these works is to demonstrate the *pure* hydrodynamic turbulence by transient growth of energy with the suitable choice of two-dimensional initial perturbation. The idea is any large growth plausibly could switch the accretion disk into the nonlinear regime which might result its subcritical transition to turbulence if energy growth exceeds the threshold for turbulence. One might argue that transient growth, even if large, can not provide much clue on the existence and properties of a turbulent basin of attraction. Schmid & Henningson (2001) and Criminale, Jackson & Joslin (2003) have described in detail that transition to turbulence is not a unique process but it depends on the initial condition/disturbance and the nature of the flow. In fact, it is known that even in presence of secondary instability linearly unstable base flows may reach to a non-

turbulent saturated state. However, turbulence definitely belongs to the nonlinear regime and it is exhibited only in the situations when large growth (or more precisely transient growth for the present purpose) switches the system over the non-linear regime. As our present goal is to understand the possible origin of hydrodynamic turbulence, we consider those situations when large transient growth governs non-linearity. At the present case where the accretion time scale is comparable (or shorter) to the time scale to achieve maximum growth (MAN), decaying nature of growth at a period longer than the accretion time scale does not matter. If growth (or maximum growth) becomes large enough that exceeds the threshold to trigger non-linearity and turbulence, then it does not matter whether growth evolves exponentially or transiently.

Dauchot & Manneville (1997) argued with a toy model that transient growth does not guaranty the transition to turbulence as the underlying phase portraits do not get deformed much in absence of any linearly unstable mode. However, that does not rule out the importance of transient growth as their model is very simplistic consisting of two variables only and growth is tinny to expect any deformation in the phase portraits. Other alternative methods were proposed to describe the subcritical transition to turbulence and then to investigate various underlying aspects in detail by e.g. Waleffe (1995, 1997), Brosa & Grossmann (1999), Waleffe (2003), Kerswell (2005), while last two works, that discuss non-rotating Couette flows and pipe flows respectively, are mostly relevant for the astrophysical purpose. Although the works bring some new insight into the subject, the main problem i.e. to understand the subcritical turbulence in three-dimension remains unsolved. This is indeed a non-trivial problem not only in astrophysics but also in fluid dynamics. In the present paper, we suggest a possible mechanism to govern non-linear effect into a Keplerian accretion disk. While our prescription does not solve the problem completely, it certainly opens up a new avenue to understand the physics behind this puzzle.

The problem with transient growth, what has been proposed as the mechanism to generate turbulence (e.g. Umurhan & Regev 2004; hereafter UR; Mukhopadhyay, Afshordi & Narayan 2005, Afshordi, Mukhopadhyay & Narayan 2005; hereafter MAN), is that in two-dimension underlying perturbations must ultimately decline to zero in the viscous flow. To overcome this limitation, it is necessary to invoke three-dimensional effects. Various kinds of secondary instability, such as the elliptical instability, are widely discussed as a possible route to self-sustained turbulence in linearly perturbed shear flows (see, e.g. Pierrehumbert 1986; Bayly 1986; Hellberg & Orszag 1988; Craik 1989; Le Diześ, Rossi & Moffatt 1996; Kerswell 2002). Therefore, we are motivated to see whether these three-dimensional instabilities are present in the Keplerian flows which consist of elliptical streamlines under two-dimensional perturbation. Goodman (1993) first explored the possible role of the elliptical instability in an accretion disk and Lubow, Pringle & Kerswell (1993) and Ryu & Goodman (1994)

showed that angular momentum may be transferred from the disk to the tidal source by the instability effect. They essentially considered the case of forced disks. Later, Ioannou & Kakouris (2001) also examined transient growth being constantly re-excited by external noise.

The three-dimensional instability of a two-dimensional flow with elliptical vortices has been demonstrated by number of authors (e.g. Craik & Criminale 1986; Waleffe 1990) and has been proposed as a generic mechanism for the breakdown of many two-dimensional high Reynolds number flows. This result motivates us to investigate whether the similar scenarios exist in a Keplerian accretion disk. Therefore, essentially we plan to investigate the Keplerian flow with two consecutive perturbation effects. The primary two-dimensional perturbation, which drives transient growth (MAN), governs elliptical streamlines in the flow. Then we consider the further three-dimensional perturbation, that is the secondary one, to this two-dimensional flow, if that drives three-dimensional instability effect in presence of viscosity. Presumably, three-dimensional instabilities lead to nonlinear feedback and self-sustained turbulence.

Although the maximum growth in the Keplerian disk with finite vertical thickness and then with finite vertical perturbation is smaller compared to that in a two-dimensional Keplerian disk, as Tevzadze et al. (2003) and MAN argued, vertical stratification may cause to have a nonvanishing asymptotic growth that is a fraction of the maximum growth. However, they could not show whether this will significantly help the onset of turbulence. By three-dimensional hydrodynamic simulations, Barranco & Marcus (2005) studied the dynamics and formation of vortices in stably stratified proto-planetary disks and found that vortices are unstable under perturbation. Theoretically, the origin of these vortices is understood as perturbation in plane shear flow (UR, MAN). Continuing in the same line of thought, recently, Umurhan et al. (2006) have shown substantial growth resulting from initial perturbations in the linearly stable steady state and have concluded that significant perturbation energy amplification occurs in accretion disks on a global scale.

In the present paper, we perform a local linear analysis in the shearing box approximation. Although a small section of an accretion disk may not reproduce the global disk properties, we assume that if turbulence is exhibited at any section, then that sustains and eventually affects the entire disk. While the local result does not guaranty its global signature, absence of local instability and then possible turbulence, perhaps, does guaranty its global absence. Therefore, from the results of this paper we can determine the future avenues of the subject, whether the analyzes for secondary instability including transient growth is a fruitful path to solve the problem.

In the next section, we outline the basic model considered for this problem describing

primary and secondary perturbation. In §3, we present the simple solution when the evolution of secondary perturbation is much rapid than that of primary one. Subsequently, in §4 we analyze the general solutions when both perturbations vary simultaneously. Finally we sum up the results with a discussion in §5.

2. The Model

We consider a small portion of the Keplerian flow centered on radius r_0 (see MAN for detail). Therefore, the Keplerian flow locally reduces to rotating Couette flow in a narrow gap limit whose unperturbed velocity vector is $\vec{U} = (0, -x, 0)$, where $x \ll r_0$. Therefore, the Navier-Stokes and the continuity equations for the dynamics of viscous incompressible disk fluid are given by

$$\frac{\partial \vec{U}}{\partial t} + \vec{U} \cdot \nabla \vec{U} + \vec{\Omega} \times \vec{\Omega} \times \hat{x} x + 2\vec{\Omega} \times \vec{U} + \nabla(\tilde{p}) = \frac{1}{R} \nabla^2 \vec{U}; \quad \nabla \cdot \vec{U} = 0, \quad (1)$$

where $\nabla = (\partial/\partial x, \partial/\partial y, \partial/\partial z)$, R is the Reynolds number, the angular frequency $\vec{\Omega} = (0, 0, 1/q)$, t is the time, and \tilde{p} is proportional to the pressure. For a Keplerian disk $q = 1.5$ and for a constant angular momentum disk $q = 2$. Here, all the variables are expressed in dimensionless units. The unit of length is the box size in the radial direction and the unit of velocity is the maximum relative velocity between two fluid elements into the box. Below we describe two subsequent perturbation effects, primary and secondary, one by one.

2.1. Primary Perturbation

Under a linear two-dimensional (primary) perturbation, the velocity vector of the (primary) flow reduces as

$$\vec{U} \rightarrow \vec{U}_p = (w_x, -x + w_y, 0) = \mathbf{A} \cdot \vec{d}, \quad (2)$$

where

$$w_x = \zeta \frac{k_y}{\kappa^2} \sin(k_x x + k_y y), \quad w_y = -\zeta \frac{k_x}{\kappa^2} \sin(k_x x + k_y y), \quad (3)$$

\mathbf{A} is a tensor of rank 2, the position vector $\vec{d} = (x, y, z)$, k_x, k_y are the components of the wave vector of perturbation, $\kappa = \sqrt{k_x^2 + k_y^2}$, and ζ is the amplitude of the vorticity perturbation. Now we concentrate on a further small patch of the primarily perturbed flow so that the spatial scale is very small compared to the wavelength of primary perturbation, $x \ll 1/k_x$,

$y \ll 1/k_y$. Therefore, \mathbf{A} comes out to be

$$\mathbf{A} = A_j^k = \begin{pmatrix} \zeta \sqrt{\epsilon(1-\epsilon)} & \zeta(1-\epsilon) & 0 \\ -(1+\zeta\epsilon) & -\zeta \sqrt{\epsilon(1-\epsilon)} & 0 \\ 0 & 0 & 0 \end{pmatrix}, \quad (4)$$

where $\epsilon = (k_x/\kappa)^2$. The above \mathbf{A} indicates the flow pattern to be a generalized elliptical one compared to that discussed in standard fluid literature (e.g. Bayly 1986; Craik 1989; Kerswell 2000) as an ordinary elliptical flow given by

$$A_j^k = \begin{pmatrix} 0 & 1-\epsilon & 0 \\ -(1+\epsilon) & 0 & 0 \\ 0 & 0 & 0 \end{pmatrix}. \quad (5)$$

2.2. Secondary Perturbation

The background flow for further perturbation (secondary one) also corresponds to eqn. (1) except \vec{U} is replaced by \vec{U}_p . The secondary perturbation modifies components of the velocity in eqn. (2) and the pressure as $\vec{U}_p \rightarrow \vec{U}_p + \vec{u}$ and $\tilde{p} \rightarrow \tilde{p} + p$. The perturbation is considered to be plane wave typed given by

$$(u_i, \tilde{p}) = (v_i(t), p(t)) \exp(ik_m(t)x^m), \quad (6)$$

where $k_m \gg k_x, k_y$. The Latin indices run from 1 to 3 such that e.g. $x^m \equiv (x, y, z)$, and thus the background velocity can be written as $U_{pi} = A_i^m x_m$. Therefore, from eqns. (1), (4) and (6) with replacing \vec{U} by \vec{U}_p and after some algebra, we obtain the evolution of a linear secondary perturbation

$$\dot{v}_j + A_j^k v_k + 2 \epsilon_{mkj} \Omega^m v^k = -ip k_j - \frac{v_j}{R} k^2, \quad (7)$$

along with

$$k_n \dot{v}^n = 0, \quad \dot{k}_j = -(A_j^m)^T k_m, \quad k_n \dot{v}^n = k_m A_n^m v^n, \quad (8)$$

where the ‘over-dot’ indicates a derivative with respect to t , ϵ_{mkj} is a Levi-Civita tensor, and $k^2 = k_m k^m$.

Two components, k_1 and k_2 , of the wave-vector [$\vec{k} = k_m = (k_1, k_2, k_3)$] of secondary perturbation oscillate in time with the angular frequency $\varpi = \sqrt{\zeta(1-\epsilon)}$ at a fixed ϵ , while the third one, k_3 , remains constant. As we choose the signature of the background Minkowski space-time to be $[-, +, +, +]$, it does not matter whether any Latin index appears as a lower

case or an upper case. For example, $A_j^k = A_{jk}$, where j and k respectively indicate the row and the column number.

Now projecting out eqn. (7) by $P_i^j = \delta_i^j - k^{-2}k^j k_i$ and using eqn. (8) we obtain

$$\dot{v}_i = \left(2 \frac{k^j k_i}{k^2} - \delta_i^j \right) A_j^k v_k - 2 \epsilon_{mki} \Omega^m v^k - \frac{v_i}{R} k^2 + \left(2 \epsilon_{mkj} \Omega^m v^k + \frac{v_j}{R} k^2 \right) \frac{k^j k_i}{k^2}. \quad (9)$$

A similar equation was obtained by Bayly (1986), except that they now have additional terms induced due to the Coriolis and the viscous effects.

As R is very large in an accretion disk, we neglect the viscous term in eqn. (9) comparing with others and rewrite the equation as

$$\dot{v}_i = \Lambda_{ij}^j v_j, \quad (10)$$

where

$$\Lambda_{ij} = \begin{pmatrix} \left(\frac{2k_1^2}{k^2} - 1 \right) A_{11} + \frac{2k_1 k_2}{k^2} \left(A_{21} + \frac{1}{q} \right) & \frac{2k_1^2}{k^2} \left(A_{12} - \frac{1}{q} \right) + \frac{2}{q} - A_{12} + \frac{2k_1 k_2}{k^2} A_{22} & 0 \\ \frac{2k_1 k_2}{k^2} A_{11} + \frac{2k_2^2}{k^2} \left(A_{21} + \frac{1}{q} \right) - A_{21} - \frac{2}{q} & \frac{2k_1 k_2}{k^2} \left(A_{12} - \frac{1}{q} \right) + \left(\frac{2k_2^2}{k^2} - 1 \right) A_{22} & 0 \\ \frac{2k_1 k_3}{k^2} A_{11} + \frac{2k_2 k_3}{k^2} \left(A_{21} + \frac{1}{q} \right) & \frac{2k_1 k_3}{k^2} \left(A_{12} - \frac{1}{q} \right) + \frac{2k_2 k_3}{k^2} A_{22} & 0 \end{pmatrix}. \quad (11)$$

We essentially need to solve eqn. (10) to demonstrate the behavior of perturbations. Next we describe the solution in various possible situations.

3. Perturbation Solution at a fixed ϵ

The solution with constant ϵ ¹ implies the result at a particular instant of the evolution of primary perturbation that provides the *instantaneous growth rate*. The underlying idea is to focus on the situation when the evolution of secondary perturbation and the corresponding development of growth is much rapid compared to that due to primary perturbation and therefore ϵ practically remains constant during secondary perturbation evolution. This helps us to compare the result with what exists in standard fluid literature (e.g. Bayly 1986; Kerswell 2002).

The general solution of eqn. (10) can be written as a linear superposition of Floquet modes

$$v_i(t) = \exp(\sigma t) f_i(\phi), \quad (12)$$

¹This is to remind that the radial wave-vector of primary perturbation, k_x , varies with t (MAN), therefore in reality the background for secondary perturbation appears to be time-dependent.

where $\phi = \varpi t$, $f_i(\phi)$ is a periodic function with time-period $T = 2\pi/\varpi$, and σ is the Floquet exponent which is the eigenvalue of the problem. Clearly, if σ is positive then perturbation increases with time. Applying the periodicity condition, $f_i(2\pi) = f_i(0)$, in eqn. (12), we obtain

$$v_i(T) = \exp(\sigma T) f_i(2\pi) = \exp(\sigma T) f_i(0) = \exp(\sigma T) v_i(0). \quad (13)$$

Therefore, $\exp(\sigma T)$ serves as an evolution operator.

To determine the exponential growth rate, 2σ , we strictly follow e.g. Bayly (1986) and Craik (1989). In this method, one has to evaluate the associated velocity evolution matrix, whose eigenvalue and eigenvector at $t = T$ are $e^{\sigma T}$ and $f_i(2\pi) = f_i(0)$ respectively, satisfying

$$\frac{dM_{ji}(t)}{dt} = \Lambda_j^m M_{mi}(t), \quad (14)$$

where $M_{ji}(0) = \delta_{ji}$. Essentially $M_{ji}(t)$ serves as an evolution operator such that

$$v_j(t) = M_{ji}(t)v_i(0). \quad (15)$$

Thus, using the fourth order Runge-Kutta method, one can easily compute the elements of the 3×3 matrix $M_{ji}(T)$. Interesting feature to note is that $\langle Tr(\Lambda_{ij}) \rangle = 0^2$ over $0 \leq t \leq T$. Therefore, $\det(M_{ji}(T)) = 1$. Moreover, $d(k_j M_i^j(t))/dt = 0$ and therefore $k_i(0) = k^j(0)M_{ji}(T)$ which indicates that one eigenvalue of this 3×3 matrix is always unity. The remaining two eigenvalues of $M_{ji}(T)$ must be either real and reciprocal to each other or complex conjugate to each other with unit modulus. This property helps us to check the accuracy of results such that the product of all three eigenvalues must be unity. Therefore, our problem reduces to evaluate two non-trivial eigenvalues, μ_1, μ_2 , of the matrix $M_{ji}(T)$. If μ_1 or μ_2 is real and positive, then the Floquet exponent $\sigma_i = \log(\mu_i)/T$.

When the initial value of \vec{k} , i.e., $\vec{k}(0) = k_m(0) \equiv (0, 0, 1)$, $\vec{k}(t)$ remains conserved throughout as follows from eqn. (8). This is the *pure* vertical perturbation. In this case, Λ_{ji} in eqn. (11) appears as a constant matrix. Therefore, $e^{\sigma t}$ and $f_i(t)$ are the eigenvalue and the eigenvector respectively of the matrix $M_{ji}(t)$ at any time t and thus the Floquet exponent can be evaluated at any instant. In fact, there is an exact analytical solution for the Floquet exponents for this initial condition which are the eigenvalues of the matrix Λ_{ji} .

²' Tr ' denotes the sum of diagonal elements of the matrix, $\langle \dots \rangle$ indicates the averaged value, and 'det' refers to the determinant of the matrix.

3.1. Ideal elliptical flow

Before investigating our accretion disk solutions in detail, let us recapitulate the nature of standard elliptical flow and the corresponding instability discussed in the fluid dynamics literature since long time. The velocity of a two-dimensional fluid element with elliptical streamlines is given by $\vec{U}_p = \mathbf{A} \cdot \vec{d}$ (see, e.g. Kerswell 2002) with the definition of \mathbf{A} as follows from eqn. (5).

Now following the perturbation technique described in §2.2, we obtain Λ_{ij} given by eqn. (11) with the components of \mathbf{A} as follows from eqn. (5). If \vec{k} is constant, i.e. perturbation is vertical, then Λ_{ij} is also a constant matrix given by

$$\Lambda_{ji} = \begin{pmatrix} 0 & 2\Omega_z + \epsilon - 1 & 0 \\ -2\Omega_z + \epsilon + 1 & 0 & 0 \\ 0 & 0 & 0 \end{pmatrix}, \quad (16)$$

whose non-trivial eigenvalues are the velocity growth rates, Floquet exponents, given by

$$\sigma = \pm \sqrt{\epsilon^2 - (1 - 2\Omega_z)^2}. \quad (17)$$

For a Keplerian flow, $\sigma = \pm \sqrt{\epsilon^2 - 1/9}$. Therefore, the vertical perturbation gives rise to the positive *instantaneous* growth rate in a Keplerian disk for $\epsilon > 1/3$. For any other perturbation, k_1 and k_2 oscillate in time with the angular frequency $\varpi = \sqrt{1 - \epsilon^2}$ and k_3 remains constant (for detailed descriptions, see, e.g. Bayly 1986; Craik 1989; Kerswell 2002). In Fig. 1, we compare the variation of maximum velocity growth rate as a function of eccentricity parameter for a Keplerian flow with that of non-rotating flow. By “maximum” we refer the quantity obtained by maximizing over \vec{k} . Clearly the growth rate is significantly large at high ϵ for a Keplerian system that is interesting for the astrophysical purpose³. This is understood physically from eqn. (17). When $\Omega_z = 0$, from eqn. (17), $\sigma = 0$ at $\epsilon = 1$. However, for a rotating flow, $\sigma = \pm 2\sqrt{q-1}/q$ at $\epsilon = 1$. This result motivates us to study the elliptical streamline (vortex) effects in an actual Keplerian flow governs in accretion disks as follows from eqn. (4).

3.2. Flow in a Keplerian disk

Here the velocity, \vec{U}_p , of the background flow (primarily perturbed flow) is defined according to \mathbf{A} given by eqn. (4). When does our primarily perturbed Keplerian flow reduce

³This is to remind that our rotating Keplerian flow described in §2 is highly eccentric at large k_x , i.e. at the early stage of the evolution of primary perturbation.

to conventional flows? (1) When $k_x \rightarrow \infty$ i.e. $\epsilon \rightarrow 1$ and $\zeta \rightarrow 1$, \mathbf{A} in eqn. (4) is same as that in eqn. (5). This is the case of an extremally eccentric flow. (2) When $k_x \rightarrow \infty$ and $\zeta \rightarrow 0$, \mathbf{A} in eqn. (4) reduces to that of plane shear flow (MAN). (3) When $k_x \rightarrow 0$ i.e. $\epsilon \rightarrow 0$ and $\zeta \rightarrow 1$, again the form of \mathbf{A} in both the equations are same. This is the case of a circular flow. (4) When $k_x \rightarrow 0$ and $\zeta \rightarrow 0$, \mathbf{A} in eqn. (4) again reduces to that of plane shear flow (MAN).

Now for a pure vertical perturbation, Λ_{ji} in eqn. (11) reduces to

$$\Lambda_{ji} = \begin{pmatrix} -\zeta\sqrt{\epsilon(1-\epsilon)} & 2\Omega_z - \zeta(1-\epsilon) & 0 \\ -2\Omega_z + \zeta\epsilon + 1 & \zeta\sqrt{\epsilon(1-\epsilon)} & 0 \\ 0 & 0 & 0 \end{pmatrix}, \quad (18)$$

where $\Omega_z = 1/q$. As before the above Λ_{ji} is a constant matrix, and thus we evaluate the Floquet exponent as

$$\sigma = \pm\sqrt{\zeta\epsilon - (2\Omega_z - 1)(2\Omega_z - \zeta)}. \quad (19)$$

Most of the works in fluid literature, so far, have been carried out for non-rotating systems without focusing on a Keplerian flow rigorously. Therefore, eqn. (19) can be seen as an extension of those results for an actual rotating Keplerian flow.

Now we understand the following points from eqn. (19). (1) When $\Omega_3 = 0$, $\sigma = \sqrt{\zeta(\epsilon - 1)}$. This verifies that non-rotating two-dimensional plane shear flow is always hydrodynamically stable under a *pure* vertical perturbation. (2) When $\Omega_3 = 1/2$, $\sigma = \sqrt{\zeta\epsilon}$. Therefore, the constant angular momentum accretion flow is always hydrodynamically unstable. The energy growth rate of perturbation increases with the strain rate i.e. the eccentricity of the flow. (3) When $\Omega_3 = 2/3$, $\sigma = \sqrt{\zeta\epsilon - (4 - 3\zeta)/9}$. Therefore, a Keplerian flow with elliptical streamlines gives rise to unbounded growth, at least in certain time interval when growth and growth rate due to primary perturbation is very small, under a *pure* vertical perturbation, only if $\zeta > 1/3$.

However, there are some other three-dimensional perturbations⁴ which can generate positive growth rate, σ , in a Keplerian flow with $\zeta < 1/3$, that we describe by numerical solutions. As primary perturbation evolves with time, eccentricity decreases, and then the energy growth rate due to secondary perturbation changes. Figure 2a shows the variation of

⁴By vertical perturbation we mean that only the vertical component of initial perturbation wave-vector is non-zero, while any other perturbation with a non-zero vertical component of initial wave-vector is called three-dimensional perturbation.

maximum growth rate, σ_{max} , as a function of eccentricity parameter, ϵ ⁵. By “maximum” we refer the quantity obtained by maximizing over the vertical component of wave-vector, k_3 . Clearly, for $\zeta < 1/3$, growth rate maximizes for three-dimensional perturbations with $k_3 < 1$. At small ϵ and large ζ , the streamlines of the flow essentially become circular (see eqn. (4)), and thus the growth rate severely decreases due to lack of significant elliptical vortex. On the other hand, when ϵ and ζ both are small, the background structure reduces to plane shear and therefore any growth arises due to primary perturbation only.

Figure 2b shows the variation of optimum growth rate, σ_{opt} , as a function of k_3 . By “optimum” we refer the quantity obtained by maximizing over ϵ . Interesting fact to note is that the optimum growth rate is always obtained for three-dimensional perturbation with significant vertical component. Moreover, as ζ increases, the best growth rate is obtained at high ϵ with large k_3 . Therefore, three-dimensional growth is more prompt at larger ζ .

4. Computation of growth with simultaneous evolution of both perturbations

Above results verify that at some parameter range the three-dimensional growth rate due to secondary perturbation in rotating shear flow is expected to be real and positive, which motivates us to analyze the simultaneous evolution of both perturbations. As primary perturbation evolves, k_x varies with time and therefore ϵ and then \mathbf{A} does so. Thus, although eqn. (8) remains still valid, in general the wave-vector of secondary disturbance is not periodic and the solution of eqn. (10) can not be expressed exactly by Floquet modes. Therefore, to compute growth in energy, one has to find out the elements of energy evolution matrix

$$\mathcal{M}_{ik}(t) = M_{im}(t)^T M_{mk}(t) \tag{20}$$

whose largest eigenvalue is growth in energy at time t . As $M_{mk}(t)$ can be obtained from eqn. (14), computation of $\mathcal{M}_{ik}(t)$ is a trivial job. The actual time variance of $\epsilon(t)$ in eqn. (14) (and in eqn. (11)) is now considered. Clearly, $\mathcal{M}_{ik}(t)$ is the instantaneous energy of perturbation of the flow, while we can remind that $M_{im}(t)$ is the instantaneous velocity of perturbation.

Figure 3 depicts the evolution of best growing secondary perturbation. It is clear that perturbation at $t = 0$ is a leading wave with a large negative k_1 (as well as k_x , although $k_x \ll k_1$) and therefore the flow is highly eccentric at the beginning. With time, k_1 (as well

⁵Note that ϵ is a parameter that carries the information of eccentricity of the system but is not the eccentricity itself.

as k_x) decreases in magnitude and finally becomes zero at $t = t_{\max}$ when growth maximizes. With further increase of time, the wave becomes trailing and growth starts to decrease.

Figure 4a shows that as ζ increases, the (first) peak value of growth increases and that occurs at an earlier time. Comparing with the variation of k_1 as a function of t , as shown in Fig. 4c, it is very clear that a peak in growth appears when k_1 approaches to zero. As k_1 in the cases with $\zeta = 0.05$ and 0.1 becomes zero twice, corresponding growth maximizes twice too. The second peak appears at $t \sim 1000$ when $k_x \sim k_1 \rightarrow 0$. Moreover, for $\zeta = 0.4$, k_1 becomes zero thrice (it cuts the zero line at $t \sim 1000$ and becomes negative, but immediately turns up and cuts the zero again). Therefore, the corresponding growth curve attains two peaks at $t \sim 1000$ very close to each other, apart from the first one at $t = 503$. The maximization of growth at the minimization of the radial component of perturbation wave vector was explained in MAN. This is essentially due to the fact that $G \propto 1/k^2$. If $\zeta = 0$, then k_1 and k_x both become zero simultaneously as shown in Fig. 4c. However for $\zeta > 0$, k_1 increases faster, as follows from eqn. (8), and becomes zero earlier than k_x . The interesting fact to note is that underlying growth, although apparently is of transient kind as shown in Fig. 4a, diverges asymptotically for any $\zeta > 1/3$, while converges for $\zeta \leq 1/3$. The asymptotic divergence of growth is similar to the instability one obtains in linear perturbation analysis for Poiseuille flow at $R \gtrsim 5772$ (e.g. Reddy & Henningson 1993). The significant asymmetry around $t = t_{\max}$ and non-zero asymptotic value in growth curves are due to the vertical structure. Figure 4b shows the variation of peak growth as a function k_3/k_2 . The quantity k_3/k_2 carries information of how three-dimensional the flow is. It is interesting to note that the maximum growth for $\zeta > 1/3$ is unbounded so that increases with vertical structure, while it is bounded for $\zeta \leq 1/3$. We know that in a two-dimensional flow, the maximum growth, G_{max} , scales with k_{x0}^2 (MAN). However for $\zeta > 0$, G_{max} decreases at small k_3/k_2 but increases at large k_3/k_2 , compared to that for $\zeta = 0$. At around $k_3/k_2 = 0.5$, which corresponds to the marginally two-dimensional perturbation, growth due to secondary perturbation is comparable to that of primary perturbation. This verifies that secondary perturbation can govern significant transient growth in a geometrically thin accretion disk with finite vertical thickness. However, in three-dimension, when $k_3/k_2 \sim 1$, the secondary perturbation effect always dominates over the primary one. This indicates that three-dimensional secondary perturbation enhances energy growth and thereafter any possible non-linear feedback effects with its elliptical base state. As k_{x0} and k_{10} ($\sim R^{1/3}$, see UR, MAN) increase, the vertical structure plays more effective roles to govern growth. When $k_{x0} = k_{10}/10 = -10^3$ and $k_y = k_{20}/10 = 1$, $G_{max} \sim 4 \times 10^4$ at $k_3/k_2 = 1$ for $\zeta = 0.1$, which is an order of magnitude larger compared to that for $\zeta = 0$. If we consider a smaller R with $k_{x0} = k_{10}/10 = -10^2$, then G_{max} at $k_3/k_2 = 1$ decreases to $\sim 2 \times 10^3$ for $\zeta = 0.1$, which is still larger by a factor of two compared to that for $\zeta = 0$. Therefore, three-dimensional effects efficiently enhance

growth and then presumably help to trigger turbulence in shear flows.

5. Discussions

We find that significant energy growth of perturbation is possible to govern in shear flow with the Coriolis force. This system is an idealized local analog of an accretion disk which, under secondary perturbation, definitely exhibits three-dimensional large growth of transient kind and, in addition, sometimes exhibits unbounded late-time growth at a large amplitude of primary perturbation. We have explicitly demonstrated the perturbation effects one by one. First, primary two-dimensional perturbation induces vortex into the flow that can be locally seen as elliptical streamlines. This system, which does not have any exponential growing eigenmode but does exhibit significant transient growth, has been extensively studied already (e.g. UR; Yecko 2004; MAN). In this situation, a plane wave perturbation, that is frozen into the fluid, is sheared along with the background flow. At $t = 0$, the effective wave vector of perturbation is in the x direction ($k_x \gg k_y$) and is negative which provides very asymmetric leading waves. Therefore, the flow at this stage is highly eccentric. As time goes on, the wavefronts are straightened out by the shear and $|k_x|$ decreases and transient growth increases. When $k_x \sim 0$, i.e. the wavefronts become almost radial, transient growth is maximum. At this time, the streamlines of the flow are almost circular. At yet later time, growth decreases and the wave becomes trailing. Then it has been argued that if the maximum growth exceeds the threshold for inducing turbulence, then this mechanism could drive the system to a turbulent state. Presumably, once the system becomes turbulent, it remains turbulent as a result of nonlinear interactions and feedback among the perturbations. It can be reminded that our present aim is to understand and establish the origin of viscosity in the flow that must be due to turbulence. The transfer of mass inward and angular momentum outward in an accretion disk is difficult to explain in absence of turbulence. However, the accretion disk is quite a complex system with, possibly, continuous perturbed flow. Therefore, if we can address a mechanism to govern turbulence, then its recycling is not a difficult job.

Second, we consider further perturbation, namely secondary perturbation, into the flow described above. The primarily perturbed shear flow serves as a background for secondary perturbation whose eccentricity naturally varies with time due to the evolution of primary perturbation. In this paper, we have especially demonstrated the evolution of this secondary perturbation which exhibits three-dimensional large transient growth in a local Keplerian accretion disk. While primary perturbation itself can produce large transient growth at a high Reynolds number that might drive the non-linear effects into the system, the best

perturbation responsible for this effect is two-dimensional. However, it is understood that perturbations must ultimately decline to zero in presence of viscosity (see e.g. UR), unless three-dimensional effects are invoked. Therefore, we have addressed the possible origin of three-dimensional effects that shows a clear route to three-dimensional hydrodynamic growth and then possible non-linear feedback and turbulence in accretion flows. Underlying growth arises due to the elliptical vortices present in the background, rather than due to the plane shear which exhibited growth under primary perturbation.

In the standard fluid literature, the elliptical instability has been widely discussed as a possible route to self-sustained turbulence in linearly perturbed shear flows, as mentioned in §1. However, usual emphasis of those investigations is on non-rotating flows. Craik (1989), while discussed about the elliptical instability in rotating shear flows, did not focus on a Keplerian flow, what is of astrophysical interest. Therefore, in the present paper, we have first discussed the growth rate in standard elliptical flows and compared the results for non-rotating flows with that of rotating ones in §3.1. We have shown that the growth rate in a Keplerian flow with constant elliptical streamlines is significantly large compared to that in a non-rotating flow, particularly at high eccentricity.

However, in reality, when a small section of a Keplerian accretion disk is considered under a two-dimensional linear perturbation, the flow governs distorted elliptical streamlines whose structure vary with time. Therefore, the growth rate due to secondary perturbation at a fixed ϵ (instantaneous growth rate) as described in §3.2 decreases much compared to that in the flow with idealized elliptical streamlines, unless the amplitude of primary perturbation, ζ , is very large. At a $\zeta > 1/3$, a pure vertical secondary perturbation produces the best growing eigenmode. On the other hand, at a $\zeta \leq 1/3$, the best growing eigenmode arises due to other three-dimensional perturbations with a significant, but not sole, vertical effect. Although the instantaneous growth rate appears to be small for a small ζ (which is of particular interest), at least compared to the case with idealized elliptical streamlines, actual growth which is the result of simultaneous evolution of both perturbations as described in §4 can be large enough to exhibit non-linear effects if the time-scale for the evolution of perturbation is large. The time for the evolution of perturbation scales with the Reynolds number of the flow as $R^{1/3}$ (MAN). As perturbation evolves, k_x varies from $-\infty$ to 0 and thus the eccentricity of the flow decreases from 1 to 0. Most of the important three-dimensional growing modes are generated at the high eccentricity regime when $0.995 \leq \epsilon \leq 1$ and therefore $10 \leq |k_x| \leq \infty$. Important fact to note is that growth maximizes for three-dimensional perturbation with a significant vertical effect.

We therefore conclude with an important caveat. UR already showed via two-dimensional simulations that chaotic motions can persist for a time much longer than the time scale

needed for linear growth. However, the corresponding vorticity decays unless the vertical structure is there. In the present paper, we have shown the existence of three-dimensional perturbation effects and corresponding eigenmodes which governs large energy growth and then suggests the possible existence of non-linear effects and self-sustained hydrodynamic turbulence in accretion disks. Now one will have to verify our suggestion by numerical simulation with proper resolution and possibly also by nonlinear analytic asymptotic methods.

The author is grateful to Ramesh Narayan for suggesting this problem and for extensive discussion and encouragement throughout the course of the work. The author is also thankful to the referee for his/her constructive suggestions that help to improve the presentation of the paper. This work was supported in part by NASA grant NNG04GL38G and NSF grant AST 0307433.

REFERENCES

- Balbus, S. & Hawley, J. 1991, *ApJ*, 376, 214.
- Balbus, S., Hawley, J., & Stone, J. 1996, *ApJ*, 467, 76.
- Barranco, J. & Marcus, P. 2005, *ApJ*, 623, 1157.
- Bayly, B. 1986, *Phys. Rev. Lett.*, 57, 2160.
- Blaes, O. & Balbus, S. 1994, *ApJ*, 421, 163.
- Brosa, U. & Grossmann, S. 1999, *Euro. Phys. J. B*, 9, 343.
- Butler, K. & Farrell, B. 1992, *Phys. Fluids A*, 4(8), 1637.
- Chagelishvili, G., Zahn, J.-P., Tevzadze, A. & Lominadze, J. 2003, *A&A*, 402, 401.
- Craik, A. 1989, *J. Fluid Mech.*, 198, 275.
- Craik, A. & Criminale, W. 1986, *Proc. R. Soc. London Ser. A*, 406, 13.
- Criminale, W. O., Jackson, T. L., & Joslin, R. D. 2003, *Theory and Computation in Hydrodynamic Stability* (Cambridge: Cambridge Univ. Press).
- Dauchot, O., & Manneville, P. 1997, *J. Phys. II France*, 7, 371.
- Gammie, C. & Menou, K. 1998, *ApJ*, 492, L75.

- Goodman, J. 1993, *ApJ*, 406, 596.
- Hawley, J., Balbus, S., & Winters, W. 1999, *ApJ*, 518, 394.
- Hellberg, C., & Orszag, S. 1987, *Phys. Fluids*, 31(1), 6.
- Ioannou, P. J., & Kakouris, A. 2001, *ApJ*, 550, 931.
- Johnson, B., & Gammie, C. 2005, *ApJ*, 626, 978.
- Kerswell, R. 2002, *Ann. Rev. Fluid Mech.*, 34, 83.
- Kerswell, R. 2005, *Nonlinearity*, 18, R17.
- Le Diześ, S., Rossi, M. & Moffatt, K. 1996, *Phys. Fluids*, 8(8), 2084.
- Lesur, G., & Longaretti, P.-Y. 2005, *A&A*, 444, 25.
- Longaretti, P.-Y. 2002, *ApJ*, 576, 587.
- Lubow, S., Pringle, J., & Ryu, D. 1994, *ApJ* **419**, 758.
- Menou, K. 2000, *Science*, 288 (5473), 2022.
- Menou, K., & Quataert, E. 2001, *ApJ*, 552, 204.
- Mukhopadhyay, B, Afshordi, N., & Narayan, R. 2005, *ApJ*, 629, 383; Afshordi, N., Mukhopadhyay, B. & Narayan, R. 2005, *ApJ*, 629, 373; *MAN*.
- Papaloizou, J. C. B. 2005, *A&A*, 432, 743; *A&A*, 432, 757.
- Pierrehumbert, R. 1986, *Phys. Rev. Lett.*, 57, 2157.
- Reddy, S. C., & Henningson, D. S. 1993, *J. Fluid Mech.*, 252, 209.
- Richard, D., & Zahn, J.-P. 1999, *A&A*, 347, 734.
- Ryu, D., & Goodman, J. 1994, *ApJ*, 422, 269.
- Schmid, P. J., & Henningson, D. S. 2001, *Stability and Transition in Shear Flows* (New York: Springer-Verlag).
- Shakura, N., & Sunyaev, R. 1973, *A&A*, 24, 337.
- Tevzadze, A., Chagelishvili, G., Zahn, J.-P., Chanishvili, R., & Lominadze, J. 2003, *A&A*, 407, 779.

Trefethen, L., Trefethen, A., Reddy, S. & Driscoll, T. 1993, *Science*, 261, 578.

Umurhan, O., Nemirovsky, A., Regev, O., & Shaviv, G. 2006, *A&A*, 446, 1.

Umurhan, O., & Regev, O. 2004, *A&A*, 427, 855; UR.

Waleffe, F. 1990, *Phys. Fluids A*, 2, 76.

Waleffe, F. 1995, *Phys. Fluids*, 7, 3060.

Waleffe, F. 1997, *Phys. Fluids*, 9, 883.

Waleffe, F. 2003, *Phys. Fluids*, 15, 1517.

Yecko, P. 2004, *A&A*, 425, 385.

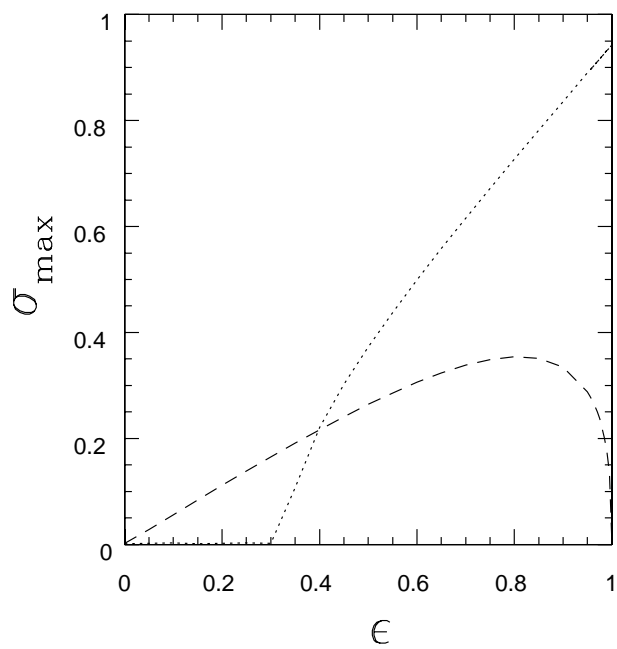


Fig. 1.— Variation of maximized growth rate for elliptical instability as a function of eccentricity parameter. Dashed and dotted curves correspond to results for non-rotating and rotating shear flows respectively. $q = 1.5$.

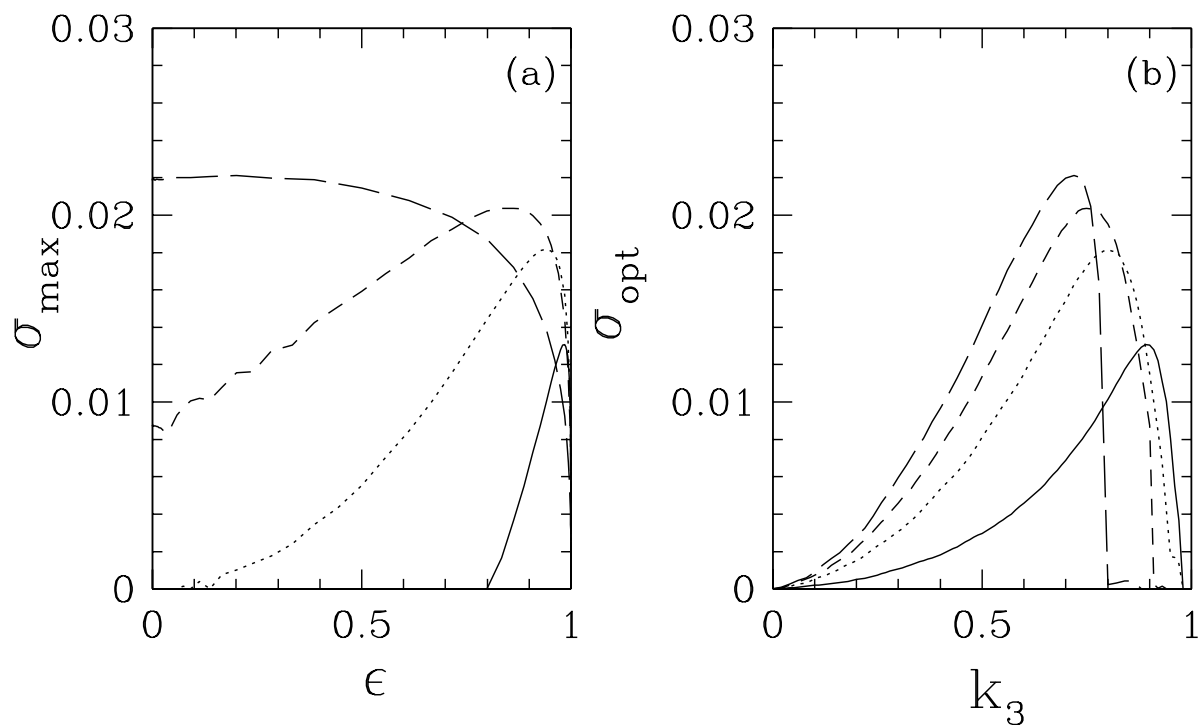


Fig. 2.— (a) Variation of maximum growth rate as a function of eccentricity parameter when solid, dotted, dashed and long-dashed curves indicate the results for $\zeta = 0.2, 0.1, 0.05, 0.01$ respectively. (b) Variation of optimum growth rate as a function of vertical component of perturbation wave-vector when various curves are same as of (a). $q = 1.5$, $|\vec{k}_0| = 1$ throughout.

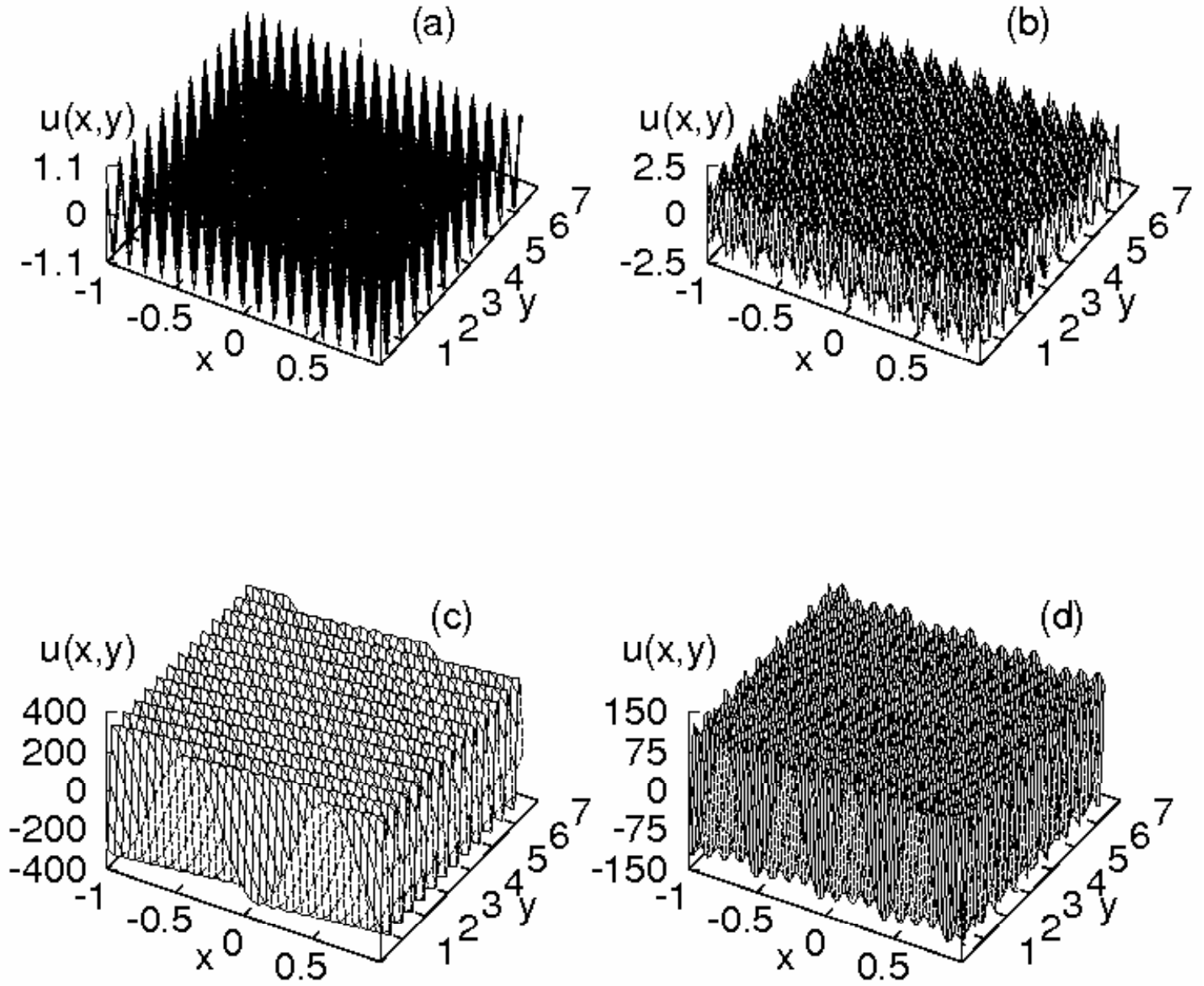


Fig. 3.— Evolution of secondary perturbation in the x - y plane for $\zeta = 0.1$, when (a) $t = 0$, (b) $t = t_{\max}/2 = 386$, (c) $t = t_{\max} = 772$, (d) $t = 3t_{\max}/2 = 1158$. Other parameters are $k_{x0} = k_{10}/10 = -1000$, $k_y = k_{20}/10 = 1$, $k_3 = 10$, and $q = 1.5$. The perturbation is normalized by the magnitude of that at $t = 0$.

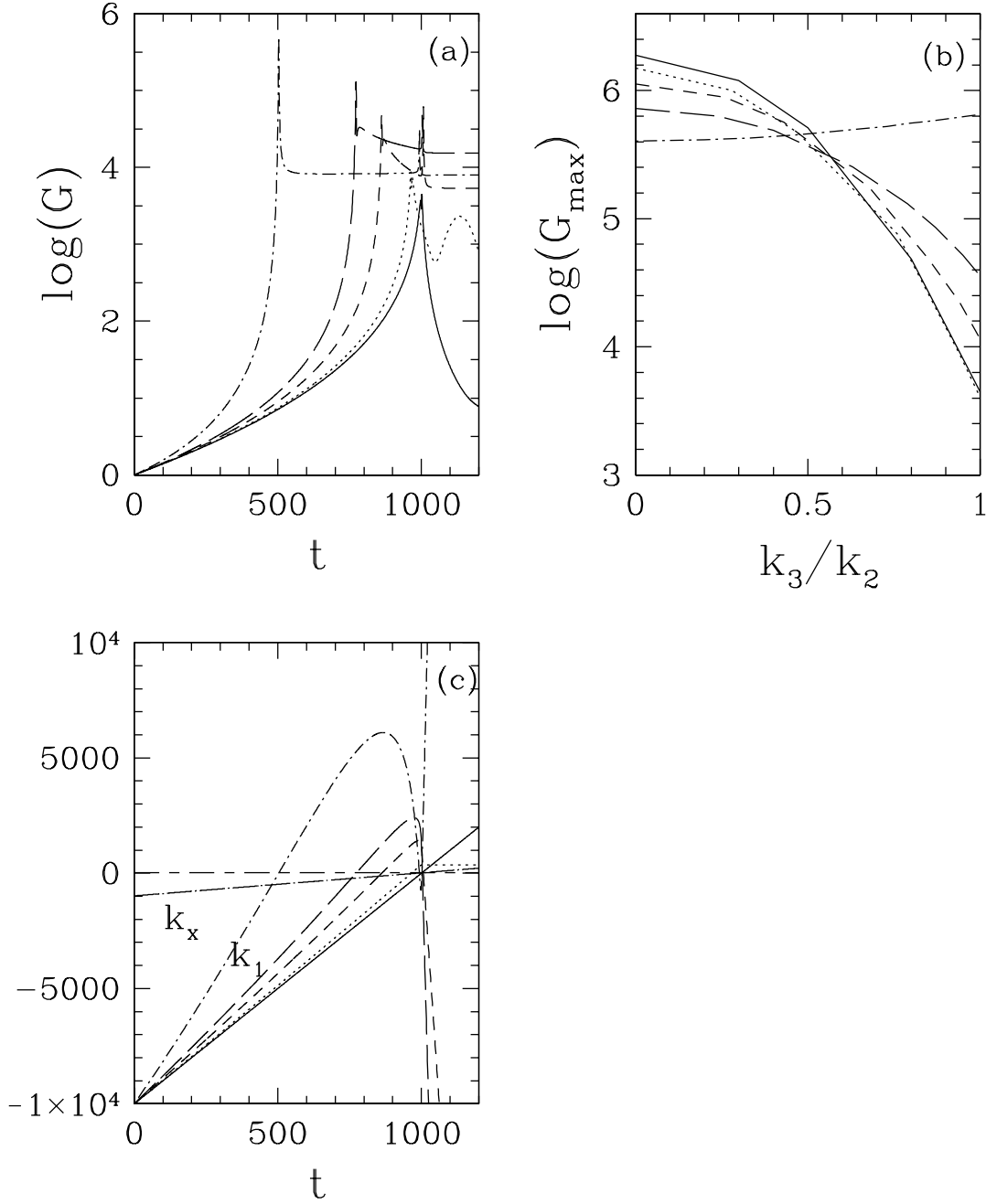


Fig. 4.— (a) Variation of growth as a function of time due to simultaneous evolution of both perturbations, when $k_3 = 10$. Solid, dotted, dashed, long-dashed and dot-dashed curves indicate the results for $\zeta = 0, 0.01, 0.05, 0.1, 0.4$ respectively. (b) Variation of maximum growth as a function of k_3/k_2 , when various curves are same as of (a). (c) Variation of radial component of primary (k_x ; dot-long-dashed curve) and secondary (k_1 ; curves have same meaning as of (a)) perturbation as functions of time, of the cases in (a). The dashed-long-dashed curve indicates the line with zero value of the wave vector. Other parameters are $k_{x0} = k_{10}/10 = -1000$, $k_y = k_{20}/10 = 1$, and $q = 1.5$. Note the change in behavior of curves, particularly in (b), when $\zeta > 1/3$.